Adaptive Array Processing for GPS Interference Rejection

David S. De Lorenzo, *Stanford University*
Jennifer Gautier, *Stanford University*
Jason Rife, *Stanford University*
Per Enge, *Stanford University*
Dennis Akos, *University of Colorado at Boulder*

BIOGRAPHY

David De Lorenzo is a member of the Stanford University GPS Laboratory, where he is pursuing a Ph.D. degree in Aeronautics and Astronautics. He received a Master of Science degree in Mechanical Engineering from the University of California, Davis, in 1996. David has worked previously for Lockheed Martin and for the Intel Corporation.

Dr. Jennifer Gautier is currently the Institute of Navigation Executive Fellow for 2005-2006. Previously, Dr. Gautier was a Research Associate in the GPS Laboratory at Stanford University, where she led the Lab's research program for the Joint Precision and Approach Landing System (JPALS). She received the Bachelor's degree in Aerospace Engineering from Georgia Tech and completed the Master's and Ph.D. degrees in Aeronautics and Astronautics at Stanford University. Dr. Gautier has worked for Lockheed, Honeywell Labs, and Trimble Navigation, Ltd.

Dr. Jason Rife is a Research Associate studying JPALS and the Local Area Augmentation System (LAAS) at Stanford University. After receiving his B.S. in mechanical and aerospace engineering from Cornell University (1996), he spent one year working in the turbine aerodynamics group of the commercial engine division of Pratt & Whitney. He resumed his studies at Stanford and earned M.S. (1999) and Ph.D. (2004) degrees in mechanical engineering. His thesis work focused on positioning and navigation technologies for underwater robots.

Dr. Per Enge is a Professor of Aeronautics and Astronautics at Stanford University, where he is the Kleiner-Perkins, Mayfield, Sequoia Capital Professor in the School of Engineering. He directs the GPS Research Laboratory, which develops satellite navigation systems based on the Global Positioning System. Dr. Enge has received the Kepler, Thurlow, and Burka Awards from the Institute of Navigation for his work. He is a Fellow of the Institute of Navigation and the Institute of Electrical and Electronics Engineers.

Dr. Dennis M. Akos is an Assistant Professor with the Aerospace Engineering Science Department at the University of Colorado at Boulder. He also has served as a faculty member with the Luleå Technical University, Sweden, and as a Research Associate in the GPS Laboratory at Stanford University. Dr. Akos completed the Ph.D. degree in Electrical Engineering at Ohio University within the Avionics Engineering Center.

ABSTRACT

One area of active interest in the GNSS community is determining the vulnerability of multi-antenna signal processing algorithms given calibration errors in antennas and analog front-end hardware. Errors introduced by the antennas or by the analog hardware that are not completely mitigated by software or calibration may lead to degradation in steering-vector accuracy. Of interest are the characterization and mitigation of any consequent reduction in C/N_0 and biasing of code and carrier phase estimates. When a reference signal is available (as is the case for GPS) and when there may be degradation in steering-vector accuracy (due to hardware errors), then an adaptive mean-square-error based approach may have significant C/N_0 advantages. Further, exercising both spatial and temporal degrees of freedom is desirable in maximizing C/N_0 for adaptive antenna arrays. Stanford University's multi-channel hardware testbed demonstrates the feasibility of implementing adaptive array processing for GPS signals in real time.

INTRODUCTION

The Joint Precision and Approach Landing System (JPALS) is a United States Navy and Air Force program to provide local-area augmentation to the on-board GPS navigation solution for pilots on approach to aircraft

carrier, fixed base, and tactical airfields. Sea-based JPALS provides carrier-phase differential navigation and as such, there is the requirement to maintain high-integrity GPS measurements while rejecting interference and multipath.

There are a broad range of interference mitigation techniques described in the literature, including antenna design changes to suppress low-elevation signals, filtering and signal processing to reduce interference power, and changes to the tracking loops including augmentation by inertial measurements [1]. One of the technologies being studied for JPALS is a controlled reception pattern antenna (CRPA) array.

The baseline JPALS architecture involves a multi-element antenna array to increase available signal-to-interference-plus-noise ratio (SINR); an additional component likely would be adaptive beamforming and nullsteering to further improve interference rejection. The sub-meter accuracy required for carrier landings necessitates limitations on navigation errors due to signal distortion, channel-to-channel timing differences, and low carrier-to-noise ratio (C/N_0).

Non-adaptive spatial-only beamforming, combined with knowledge of platform attitude and satellite constellation ephemeris, is suitable for increasing the C/N_0 of desired satellite signals. The drawbacks to this approach are high sidelobes, the requirement at all times for accurate knowledge of platform orientation and satellite ephemeris, and the susceptibility to antenna and analog front-end timing and distortion errors. However, with suitable interference detection and localization processing, a nullsteering array can significantly reduce sidelobe gain in the direction of interference sources.

Adaptive processing for noise-rejection or power-minimization allows the automatic suppression of narrowband interference and jamming, and introduces no further frequency-dependent phase distortion on the spread-spectrum GPS ranging signal [2-3]. Greater interference rejection, particularly of wideband sources, may be realized by incorporating temporal filtering in the array processing – e.g., with a tapped delay line antenna array. However, adding time taps to allow space-time adaptive processing (STAP) yields a finite impulse response filter that may distort the spread-spectrum GPS ranging signal.

The topic of multi-element steered beam and adaptive antenna arrays has received attention within the GPS community, including its impacts upon the carrier and code phase observables [e.g. 4-12]. Errors in the calibration of antennas and front-end components can introduce additional, uncompensated phase and group delay on the incoming satellite signals. The resulting impact to steering-vector accuracy, effective signal-to-noise ratio, and code and carrier phase estimation errors has not been adequately examined within the context of adaptive antenna arrays. This paper quantifies the effects to signal-to-noise ratio due to calibration errors in the antennas and front-end components, and explores the sensitivity to spatial and temporal degrees of freedom within the array.

In this paper, it is shown that when a reference signal is available (as is the case for GPS) and when there may be degradation in steering-vector accuracy (due to hardware errors), then an algorithm that minimizes the mean-square-error between the actual array output and the ideal array output may have significant C/N_0 advantages. Further, it is shown that exercising both spatial and temporal degrees of freedom is desirable in maximizing C/N_0.

To verify that the methods that are developed and tested in simulation are applicable to real-world scenarios, Stanford University has pursued construction of a data-collection hardware testbed. This testbed is based on inexpensive, commercially available front-end components and high-speed/high-resolution analog-to-digital converter cards. This testbed allows collection of high-quality signal-plus-jamming data records for subsequent playback through a variety of software tools, tracking loops, and specialized software navigation receivers.

ADAPTIVE ALGORITHMS FOR GPS

The following section presents an overview of adaptive algorithms, particularly as they apply to GPS signal processing. This brief review motivates the remainder of the discussion on antenna and analog front-end calibration errors, and spatial and temporal degrees of freedom.

For a deterministic antenna array with maximum gain achieved for a particular incoming signal vector, weights are calculated given knowledge of antenna baselines and incoming signal azimuth/elevation (and antenna gain/phase response if available). The resulting array gain pattern yields maximum constructive interference in the desired direction, but the sidelobes/nulls of the array are uncontrolled and consequently may not adequately suppress radio frequency interference (RFI) or multipath. The array output signal $x(t)$ is formed as the product of the weight vector $\mathbf{W}$ times the signal vector $\mathbf{X}(t)$:

$$x(t) = \mathbf{W}^T \mathbf{X}(t) \qquad \text{(Eq. 1)}$$

In contrast to the deterministic array, the central concept of an adaptive antenna array is the use of feedback to optimize some performance index (Figure 1). The optimization criteria can be broadly classified as either

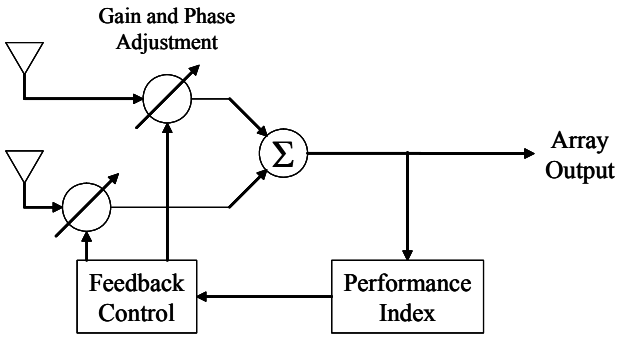

Figure 1. Generic adaptive antenna array.

maximizing the signal-to-interference-plus-noise ratio (SINR) at the array output [e.g. 13-14] or minimizing the mean-square-error (MSE) between the actual array output and the ideal array output [e.g. 15; this is termed a least-mean-square (LMS) approach]. In either case, the array adapts to maximize the desired signal and to reject interference. The optimal steady-state weight vector satisfies the Wiener solution:

$$\begin{aligned} \mathbf{W} &= \mu\mathbf{\Phi}^{-1}\mathbf{T}^* \quad \text{Applebaum} \\ \mathbf{W} &= \mathbf{\Phi}^{-1}\mathbf{S} \quad \text{Widrow LMS} \end{aligned} \qquad \text{(Eq. 2)}$$

This notation, and that used henceforth in this paper, comes from Compton, 1988. Here $\mathbf{T}^*$ is the array steering vector and $\mathbf{S}$ is the reference correlation vector. Also, note that solution of the equations in this form requires estimation and then inversion of the signal covariance matrix $\mathbf{\Phi}$, which is defined as the expected value of $\mathbf{X}^*\mathbf{X}^{\mathrm{T}}$. Estimation requires significant time-averaging (reducing the ability of the array to adapt quickly to changing signal environments) and signal buffering capacity, while inversion requires computational complexity. However, this is an approach that has been employed successfully in adaptive beamforming/nullsteering GPS architectures [e.g. 5, 8].

In recursive form, these algorithms look like:

$$\begin{aligned} \mathbf{W}_{n+1} &= \left[\mathbf{I} - \gamma\mathbf{\Phi}_n\right]\mathbf{W}_n + \gamma\mu\mathbf{T}^* \quad \text{Applebaum} \\ \mathbf{W}_{n+1} &= \left[\mathbf{I} - \gamma\mathbf{\Phi}_n\right]\mathbf{W}_n + \gamma\mathbf{S}_n \quad \text{Widrow LMS} \end{aligned} \qquad \text{(Eq. 3)}$$

With this formulation, estimation of $\mathbf{\Phi}$ may be done at each sample epoch. This form of the weight solution requires no buffering or matrix inversion, and with suitable pre-conditioning, it adapts quickly to a changing signal environment. Now, in addition to the composite signal output calculation from Eq. 1, there is the simple calculation of $\mathbf{\Phi}$ at each sample epoch (and the calculation of $\mathbf{S}$ for LMS). This also brings up an interesting characteristic of the steady-state gain pattern that results from application of an adaptive algorithm: the depths of the pattern nulls and the levels of sidelobes are optimized to balance rejection of RFI with suppression of uncorrelated noise received on each antenna channel. In other words, if the RFI power goes up, then null depth increases, while if white Gaussian noise (WGN) power goes up, then sidelobe levels go down. In short, RFI that is incident on the array is correlated across antenna elements, lending structure to the covariance matrix – this structure is suppressed by the adaptive algorithm.

As update equations, the algorithms are:

$$\begin{aligned} \mathbf{W}_{n+1} &= \mathbf{W}_n + \Delta\mathbf{W}_n \\ \Delta\mathbf{W}_n &= \gamma\left[\mu\mathbf{T}^* - \mathbf{\Phi}_n\mathbf{W}_n\right] \quad \text{Applebaum} \\ \Delta\mathbf{W}_n &= \gamma\left[\mathbf{S}_n - \mathbf{\Phi}_n\mathbf{W}_n\right] \quad \text{Widrow LMS} \end{aligned} \qquad \text{(Eq. 4)}$$

This last form is actually the most instructive – the algorithms reach steady-state when the bracketed terms in the $\Delta\mathbf{W}_n$ equations are zero, i.e., when the weight vector suppresses from the covariance matrix everything but the steering or reference vector. Of course, since only an estimate of the covariance matrix $\mathbf{\Phi}$ is available, this is an approximate solution. It is the misadjustment parameter γ (equivalent to 2μ in the treatment of Widrow and Stearns, 1985) that controls convergence speed and, as the name implies, steady-state misadjustment.

For a conventional deterministic beamsteering antenna array without signal feedback or adaptation, the required inputs to the weight control algorithm are signal arrival direction, platform orientation, and baseline geometry or array manifold (Figure 2). The Applebaum array requires an additional measure or estimate of signal covariance allowing it to control sidelobes, steer nulls, and achieve rejection of RFI. The LMS array requires signal covariance as well as an ideal array output signal; the LMS algorithm steers the array response to align the output signal with a locally-generated reference signal. For the case of adaptive array processing for GPS, this ideal array output signal is derived from the code and carrier tracking loops. Note that there does exist an ambiguity if navigation data are encoded onto the incoming signal; however, this can be addressed either by buffering of the navigation message, by suitable logic in the weight control algorithm (monitoring the polarity of the weight at the reference antenna tap), or by running in parallel two weight computations, one each for +1 and -1 data bit encoding.

ADAPTIVE ARRAY SENSITIVITY STUDY

From the previous discussion, it becomes apparent that the Applebaum array is well-suited to situations of known signal arrival direction but unknown signal waveform, whereas the LMS array is appropriate for unknown signal arrival direction but known (or correlated) reference waveform. But what happens when there are errors introduced by the hardware that are not completely

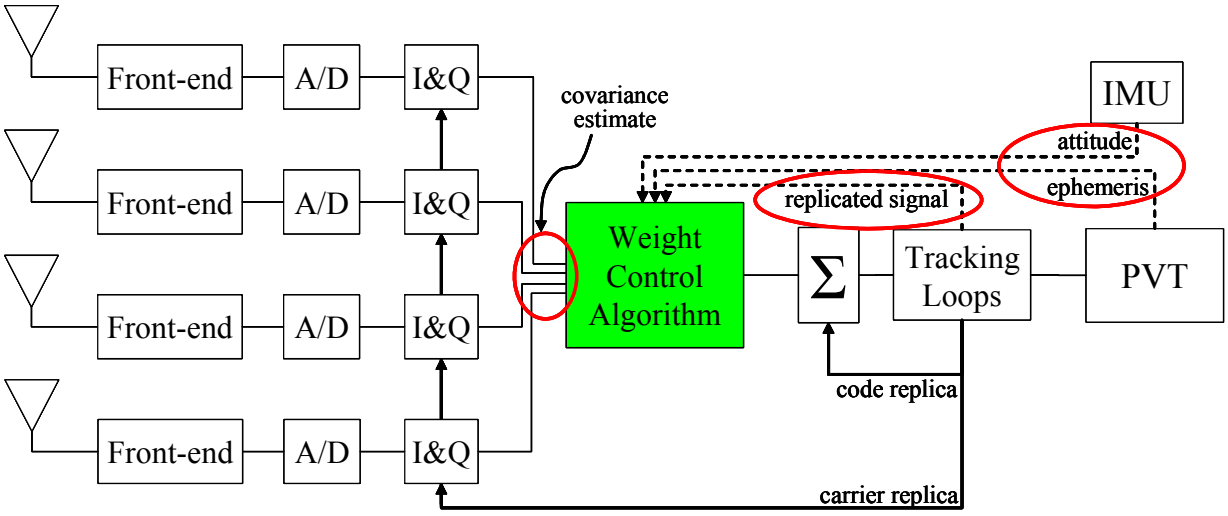

Figure 2. Inputs to weight control algorithm.

mitigated by software or calibration? These errors degrade the C/N_0 performance of steering-vector-based array schemes; however, LMS-based adaptation is robust to these effects.

To this end, a simulation study was performed to investigate the sensitivity of adaptive algorithms to varying environmental conditions. Specifically, C/N_0 was assessed for different cases, including errors and imperfections in the antenna and front-end hardware, errors in estimating the direction of arrival of the incoming signal, and the presence of RFI sources (Figure 3). This study was done for a single-element fixed reception pattern antenna (FRPA), as well as for a 7-antenna array in which signals were combined either by a deterministic controlled reception pattern antenna (CRPA) beamforming solution, by a steering-vector approach (Applebaum array), or by an algorithm that minimizes mean-square-error between the array output and a reference (LMS array). Ten satellites were placed randomly in the sky, representing C/A-code PRN sequence numbers from 1 to 10, each transmitting with a C/N_0 compared to background WGN of 50 dB-Hz; for this simulation, bandpass sampling was employed rather than mixing and downconversion to an intermediate frequency.

The bars shown in the accompanying illustration show the effective C/N_0 as reported by the GPS receiver carrier tracking loop for the previously mentioned signal combination methods (Figure 4). The text labels under each group of C/N_0 bars indicate which simulation scenario is represented: "base" case; antenna phase-center effects; phase-center, front-end, and satellite arrival errors; RFI sources present; and the "worst-case" combination with all degradation present. The superimposed vertical line on each bar graph represents ± one standard deviation from the mean. Not only is a higher C/N_0 desirable, but also a smaller standard deviation; the smaller the standard deviation, the lower the likelihood that one or more satellite signals will fall below the tracking threshold.

For the case of perfect knowledge of signal arrival direction and array orientation, no interference sources, and isotropic antennas and matched analog front-ends, it can be seen that the deterministic CRPA and the Applebaum adaptive array achieve a similar improvement in C/N_0 versus the single-element FRPA; this is to be expected, since the Applebaum array in this case uses as a steering vector the weights calculated for the deterministic CRPA, and the white, uncorrelated nature of the incident noise requires no additional adaptation to

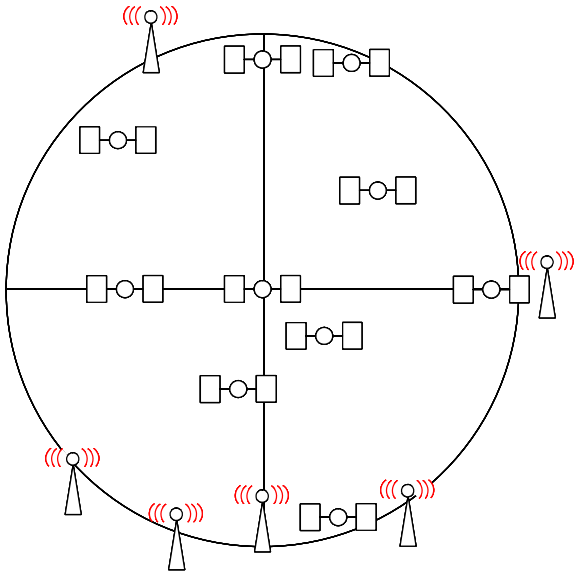

Figure 3. Satellite and RFI geometry for sensitivity study.

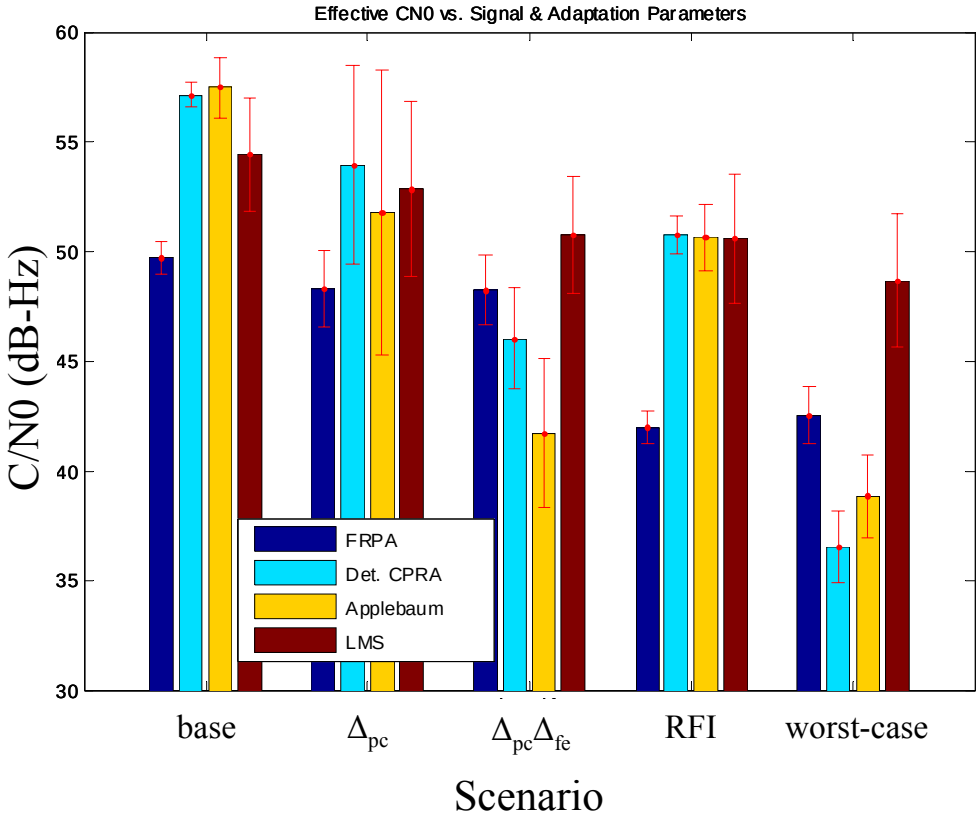

Figure 4. Adaptive array sensitivity study results.

achieve maximal SNR. There is, however, a slight penalty for the LMS array, due to gradient noise causing the converged solution to vary slightly from the ideal Wiener solution (which is equivalent to the CRPA/Applebaum weight vector solution).

Next, there is the inclusion of motion of the antenna phase-centers as a function of incoming signal arrival direction, as determined by anechoic chamber testing and computer simulation [16]. The range of advance/delay values applied to the incoming signals was ±150° of a L1 carrier cycle, and identical across all antennas. This phase-center motion causes a reduction in the C/N_0 for the CPRA and Applebaum arrays, since the steering/weight vector no longer matches the actual set of weights that would deliver maximal SNR; in other words, the effective mainbeam of the array does not coincide exactly with the actual desired incoming signal vector. The LMS array suffers no such C/N_0 degradation, as long as tracking is maintained to provide a reference waveform, since the algorithm uses in its adaptation only the desired output from the center, reference antenna element. Note that this discussion only applies to C/N_0 and signal tracking performance; biases introduced by antenna phase-center or group-delay characteristics (or analog front-end effects) also can cause code/carrier biases that would introduce errors in the navigation solution and impact the ability to successfully determine integers for carrier-phase differential RTK.

When an additional front-end differential timing delay is introduced for each antenna signal (equivalent to 0.25 wavelengths at L1, RMS with respect to the reference antenna element) as well as an error in the knowledge of signal arrival direction (2.5° RMS error in azimuth and elevation, equivalent to an equal error in platform attitude knowledge), there is further reduction in C/N_0 values. At this point, the CRPA and Applebaum arrays underperform the single-antenna FRPA system, while again the LMS array suffers little C/N_0 degradation.

The next scenario introduces six swept-CW RFI signals on or near the horizon, and each at a power level 10 dB higher than the received satellite signals, but with no other errors present in the simulation. As a note, it should be mentioned that the CW signals were swept in frequency to avoid possible lock-on from the receiver carrier tracking loop; the frequency ramp was set randomly to ±25 kHz/msec. Compared to the C/N_0 degradation seen for the FRPA, the CRPA, Applebaum, and LMS arrays all perform equally well.

Finally, the last case includes not only the six CW RFI sources, but also the antenna phase-center, front-end

delay, and signal arrival errors described above. As expected, the CRPA and Applebaum performances again fall well below that of the FRPA. The LMS array suffers no further C/N_0 degradation than for the case with RFI present only. For this scenario, the average performance of the LMS array exceeds that of the CRPA or Applebaum array by at least 10 dB-Hz.

The conclusions from this simulation study are twofold. First, in benign signal conditions, any algorithm is sufficient for signal reception; in fact, in the absence of RFI or multipath the predominant reason to employ a multi-element antenna is to increase gain toward the satellite to raise C/N_0 and improve tracking accuracy. Second, when a reference signal is available (as is the case for GPS) and when there may be degradation in steering-vector accuracy, then an LMS-based approach may have significant C/N_0 advantages.

SPATIAL AND TEMPORAL D.O.F.

In addition to the spatial degrees of freedom (d.o.f.) associated with increasing the number of antennas available for signal reception, there are temporal d.o.f. as well. By using a tapped delay line, the array synthesis may take advantage of signal information from more than one sampling epoch. Spatial d.o.f. correspond roughly with the geometry of the array gain pattern and the width (directivity/selectivity) of beams and nulls. Temporal d.o.f. are related to the spectral response of the array and the ability to null wideband RFI signals. The total d.o.f. of the array (the product of the number of antennas times the number of time taps) determines the number of beams, the depths of nulls, and may allow nulling of wideband interference. There are significant SNR benefits from a multi-antenna space-time adaptive processor (STAP) feeding into the GPS code and carrier tracking loops. In general, it is beneficial to use as many temporal d.o.f. as possible within ±½-chip of the reference tap, and within the limit established by the auto-correlation properties of the incoming sampled signal. Spatial d.o.f. can then be traded against temporal d.o.f. to reach an optimum given implementation constraints.

To examine the influence of spatial and temporal d.o.f. on GPS signal tracking performance, data were collected and then processed either from a single antenna channel or for two antennas with signals combined with an LMS adaptive algorithm. For this experiment, data were collected with two NordNav Technologies receiver front-end units operating in clock synchrony, storing 4-bit data sampled at 16.3676 MHz with a 4.1304 MHz intermediate frequency. The signals were then acquired and tracked with a software receiver implemented in Matlab™. There were 8 satellite signals present in the data records with C/N_0 values ranging from 40-49 dB-Hz.

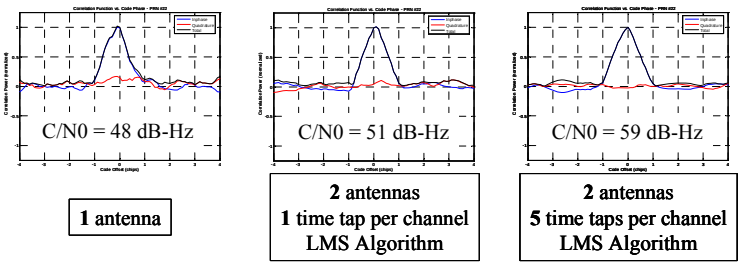

Figure 5. Tracking of C/A-code – PRN22.

For one of the satellite signals present in the data record (C/A-code for PRN22), code and carrier tracking using a single antenna channel yielded a C/N_0 estimate of 48 dB-Hz (Figure 5). When tracking the combined total of both signals, using weights determined by an LMS adaptive algorithm, the resulting C/N_0 was approximately 51 dB-Hz, a 3 dB-Hz increase, as would be expected given the increase in signal power from two antennas. It should be emphasized that these results are achieved using the desired signal as the only input to the weight control circuit – the algorithm operated "blind" in that there was no survey of antenna locations, no calculation of satellite ephemeris, no front-end or antenna calibration, and no measurement of antenna cables or front-end delays.

In contrast to the single time tap example, with a 5 time tap STAP the effective C/N_0 increased further to 59 dB-Hz, with a corresponding reduction in carrier phase and code phase errors (taps separated by $1/f_s$ = 0.061 μs). This can be thought of as being equivalent to adding equal amounts of balanced early/late multipath to the desired signal available at the center, reference time tap. The reason for the additional increase in C/N_0 is attributable to the fact that the filtered noise on the input signal (due to the receiver's analog front-end) is no longer white. As can be seen from the auto-correlation plot of a filtered WGN input sequence, there is correlation between samples; the narrower the filter passband the longer the time-extent of correlation. Since an adaptive processor uses the signal covariance matrix to drive the weight control feedback, it means that there is further noise-reduction possible with the addition of temporal d.o.f. (given a sufficiently high sampling frequency), since the independence of the input sequence has been partially eliminated. In fact, for this choice of sampling frequency there is in fact an increase in C/N_0 for a single antenna element with multiple time taps.

This effect may be more clearly seen by comparing the C/N_0 estimates for each satellite signal present in this data record (Figure 6). This plot shows estimated C/N_0 for each signal as a thin line, and tracked either with a single antenna, with both antennas and a single time tap, or with increasing numbers of time taps (3, 5, 7, 9, and 11 tap algorithms); the ensemble average is shown as the thicker, red line. These results emphasize the improvements

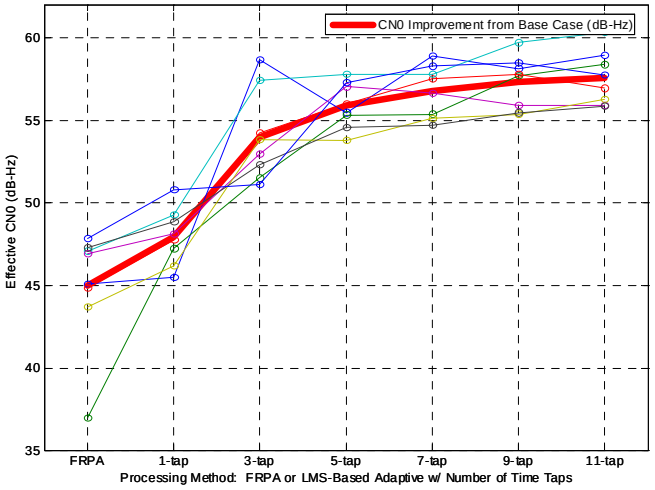

Figure 6. Estimated C/N0 with LMS-STAP.

possible by exploiting spatial and temporal d.o.f., and also show the diminishing returns as the temporal extent approaches both the ±½-chip limit as well as the time extent of the signal auto-correlation function.

An additional simulation study further examines spatial and temporal d.o.f. effects. For this simulation, the final test configuration described earlier (6 swept-CW RFI sources, antenna phase-center and analog front-end delay effects, and errors in S/V ephemeris knowledge) was used, and the number of antennas varied from 1 to 4 to 7, while the number of time taps went from 1 to 3 to 5 (Figure 7). As can be seen here, increasing either the number of antennas or the number of time taps yields increasing C/N_0. Further, even when one d.o.f. is constrained, there are still benefits to be realized by

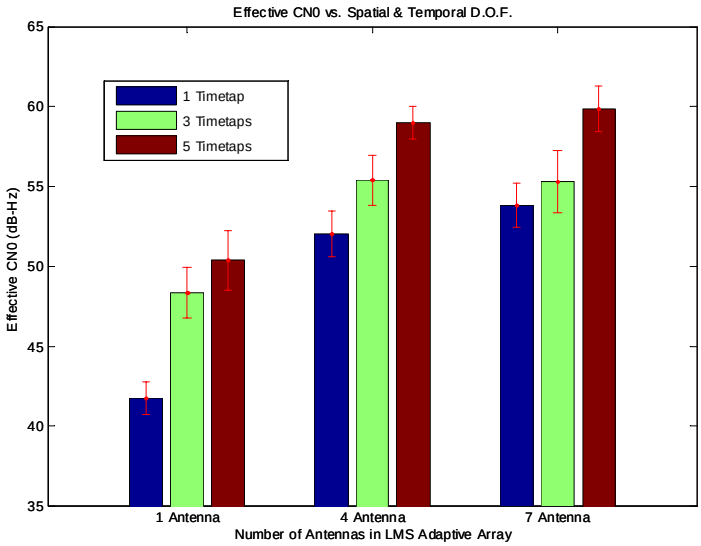

Figure 7. STAP & D.O.F. sensitivity study.

increasing the other d.o.f. Additionally, for GPS it may be functionally easier to add time taps than antennas – even with only 2 antennas, STAP will dramatically improve weak signal tracking performance.

So, mindful of practical design constraints, it is beneficial in terms of output C/N_0 to employ multiple time taps, recognizing the limits imposed by the GPS signal structure, sampling frequency, and auto-correlation properties of the sampled time series. Spatial d.o.f. can also be exercised as required to meet RFI rejection and C/N0 tracking thresholds, and given practical implementation constraints. The complementary nature of spatial and temporal d.o.f. is to be emphasized, and for maximum array performance both aspects of a design should be optimized.

STANFORD 4-CHANNEL HARDWARE TESTBED

To verify that the methods that are developed and tested in simulation are applicable to real-world scenarios, Stanford University has pursued construction of a data-collection hardware testbed. This testbed is based on inexpensive, commercially available front-end components and high-speed/high-resolution analog-to-digital converter cards. This testbed allows collection of high-quality signal-plus-jamming data records for subsequent playback through a variety of software tools, tracking loops, and specialized software navigation receivers [Figures 8 & 9; and 17-19].

Signals come in through 4 antennas placed on the roof of one of the laboratory buildings on the Stanford University campus, and are combined with an interference signal, centered at GPS L1, synthesized in the lab. These composite signals are routed to the NovAtel SuperStar II GPS cards, where they enter the analog front-end circuitry of the Zarlink GP2015 chip. The four SuperStar II GPS cards are clock synchronized by disabling their respective on-board oscillators and using instead an external 10 MHz OCXO as a timing input. After signal mixing, downconversion, and filtering on the Zarlink front-end chip, an analog IF signal is tapped from pin #1 for routing to a buffer/isolation circuit and then on to the ICS-650 A/D sampling card. The intermediate frequency from the Zarlink chip has been designed to be 4.309 MHz, so sampling at 20 MHz is more than adequate to capture the GPS C/A-coded signal bandwidth; alternatively, bandpass sampling at 5.714 MHz allows aliasing of the IF down to 1.405 MHz. Sampling is done at 12-bit A/D resolution to maximize dynamic range; this A/D resolution can be artificially degraded for study during post-processing.

Samples are stored in the on-board buffer of the A/D card with 500,000 samples per channel prior to buffer switching (which results in a data-record gap), and then written to disk. Due to the extremely large throughput of

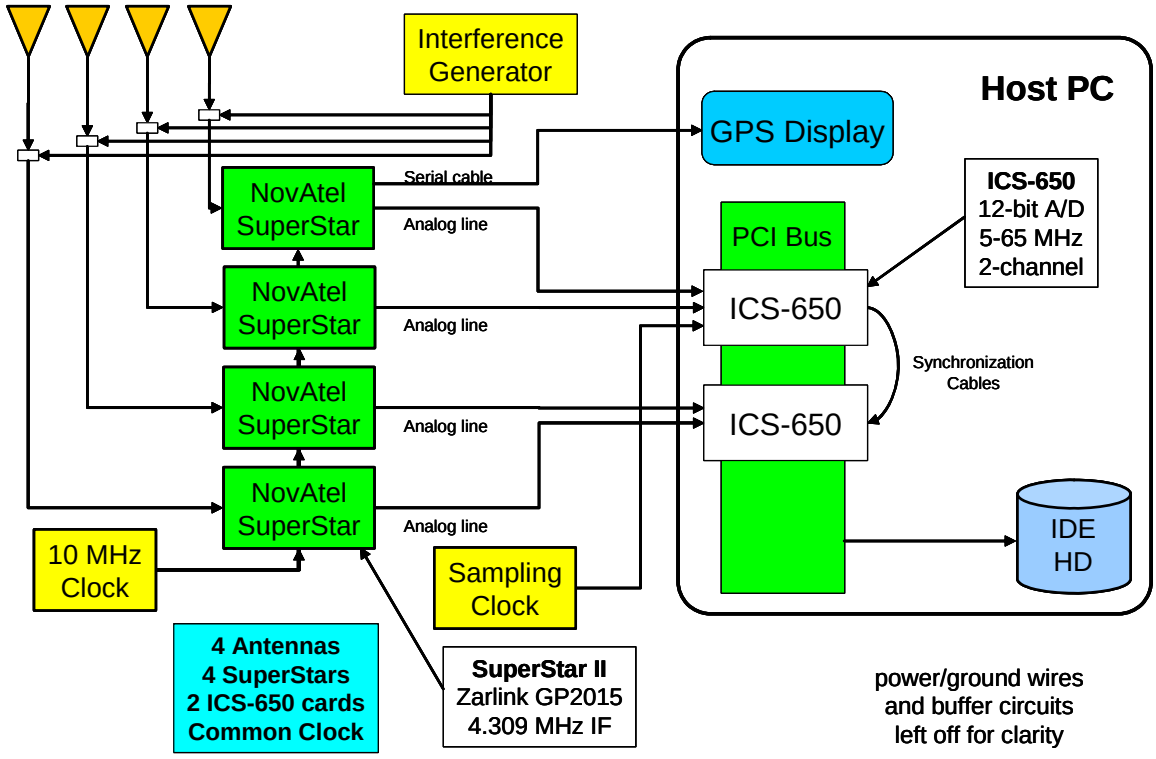

Figure 8. Stanford University 4-channel test hardware schematic.

data coming in, it has not been possible to stream the data to disk; rather, a 25-85 millisecond snap-shot is taken (depending on sampling frequency), stored on-card, and then written to disk. At this point, the saved data record is available for post-processing.

As a note, the IF signal from the GP2015 is still routed to the remainder of the SuperStar circuitry where it is processed by the on-board GPS receiver. A serial connector on the hardware chassis is utilized to connect

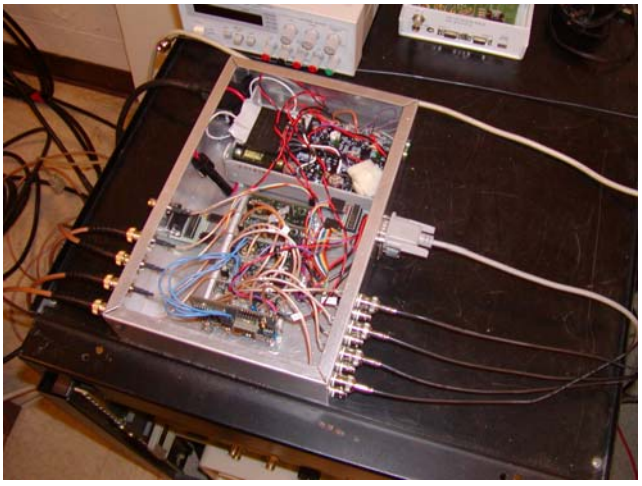

Figure 9. Stanford University 4-channel test hardware.

any of the four GPS receiver cards to the data acquisition computer, allowing easy trouble-shooting in real-time with NovAtel's StarView interface software.

An 85 ms data record was collected using the 4-channel hardware testbed sampling at 5.714 MHz. Satellite signals from each antenna were individually acquired and tracked, and also a composite signal was formed by an LMS-based adaptive algorithm and then tracked as well (using acquisition data from antenna #1). The C/N_0 for each antenna for five of the satellite signals present in the data record are shown, as well as the C/N_0 for the combined signal (Figure 10). Compared to the C/N_0 for antenna #1, which was a high-quality pinwheel antenna and had uniformly the highest C/N_0 of any antenna, the combined signal achieved an average C/N_0 improvement of 2.2 dB-Hz.

CONCLUSIONS

Multi-element antennas are an important component of the JPALS architecture, and adaptive algorithms will improve array performance in degraded conditions (interference, multipath, etc.). In this paper, it was shown that when a reference signal is available (as is the case for GPS) and when there may be degradation in steering-vector accuracy (due to hardware errors), then an LMS-based approach may have significant C/N_0 advantages. The LMS adaptive algorithm offers an efficient hardware

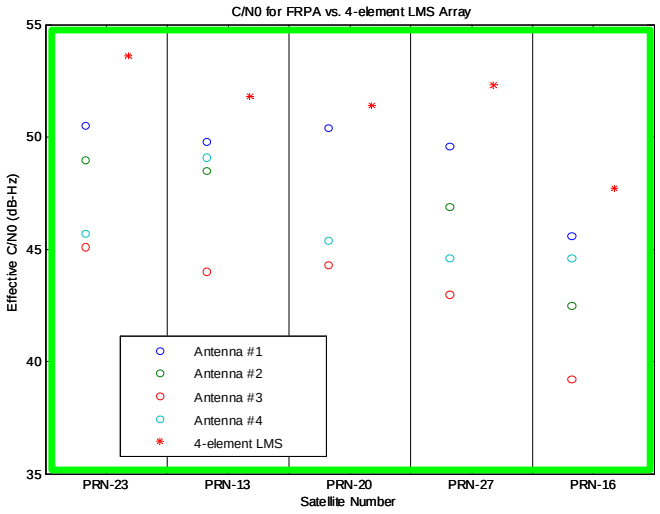

Figure 10. Signal tracking results.
PRNs 23, 13, 20, 27, 16 in dataset.

implementation, and is robust to errors in the analog electronics (Figure 11). Further, it was shown that exercising both spatial and temporal degrees of freedom is desirable in maximizing C/N_0.

This paper also included a discussion of Stanford University's multi-channel hardware testbed and an example of signal tracking results. Based on inexpensive, commercially available front-end components and high-speed/high-resolution analog-to-digital converter cards, this testbed allows collection of high-quality signal-plus-jamming data records for subsequent playback through a variety of software tools, tracking loops, and navigation receivers.

The impacts to signal tracking and pseudorange and carrier-phase estimation are strongly dependent on the errors introduced by antenna phase-center and group delay variations with incoming signal direction and also by differential propagation through the analog front-end channels. The next phase of research involves identifying compensation methods for these various effects, and determining the total impact to navigation accuracy and integrity.

ACKNOWLEDGMENTS

The authors gratefully acknowledge the invaluable electronics assistance of Gil Gutterman and Godwin Zhang in the construction of the data collection hardware described in this paper. The authors also gratefully acknowledge the support of the JPALS Program Office, and the Naval Air Warfare Center Aircraft Division through contract N00421-01-C-0022.

REFERENCES

1. Spilker, J.J. and Natali, F.D., 1996, "Interference Effects and Mitigation Techniques," in Global Positioning System: Theory and Applications, Volume I, Parkinson, B.W. and Spilker, J.J., eds., AIAA, Inc., pp 717-772.
2. Widrow, B. and Stearns, S.D., 1985, Adaptive Signal Processing, Pearson Education, Inc.
3. Compton, R.T., 1988, Adaptive Antennas, Prentice-Hall, Inc.
4. Gecan, A. and Zoltowski, M., 1995, "Power Minimization Techniques for GPS Null Steering Antenna," *Proc. ION GPS 1995*, pp. 861-868.
5. Nicholson, B.W., Upton, D.M., Cotterill, S., Marchese, J., Upadhyay, T., and Vander Velde, W.E., 1998, "Computer Simulations of Digital Beam

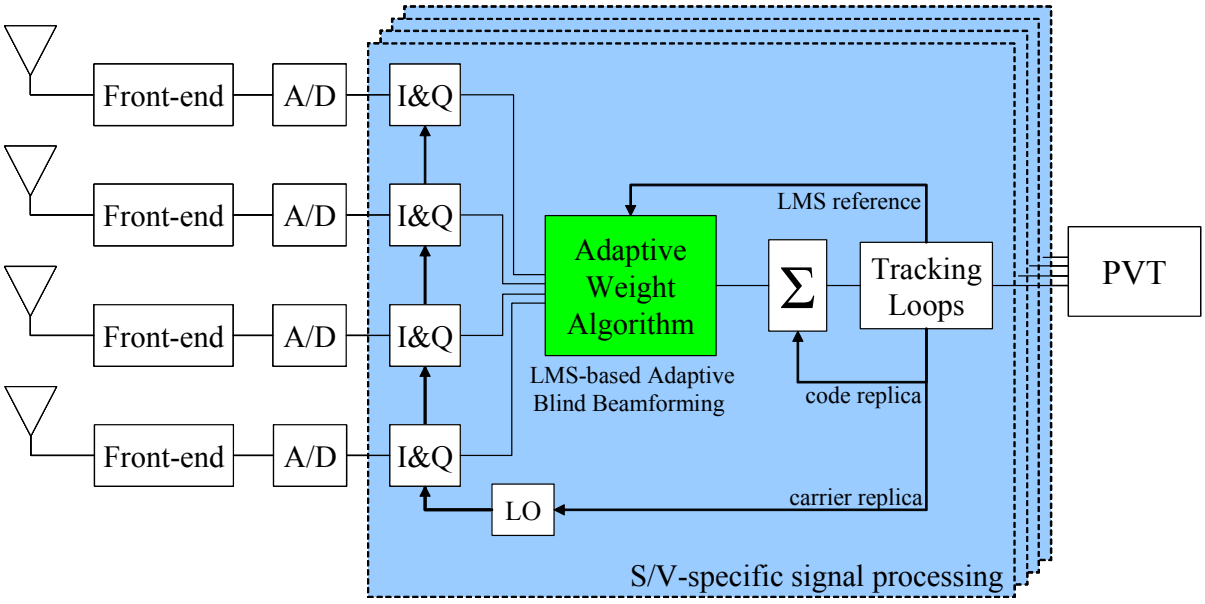

Figure 11. Proposed 1st-generation HW implementation, multi-element GPS ASIC.

Forming Adaptive Antennae for GPS Interference Mitigation," *Proc. ION NTM 1998*, pp. 355-360.
6. Hatke, G.F., 1998, "Adaptive Array Processing for Wideband Nulling in GPS Systems," *Proc. Thirty-Second Asilomar Conf. on Signals, Systems & Computers*, vol. 2, pp. 1332-1336.
7. Fante, R.L. and Vaccaro, J.J., 2000, "Wideband Cancellation of Interference in a GPS Receive Array," *IEEE Trans. on Aerospace and Electronic Systems*, vol. 36, no. 2, pp. 549-564.
8. Gupta, I.J. and Moore, T.D., 2001, "Space-Frequency Adaptive Processing (SFAP) for Interference Suppression in GPS Receivers," *Proc. ION NTM 2001*, pp. 377-385.
9. Moore, T.D., 2002, "Analytic Study of Space-Time and Space-Frequency Adaptive Processing for Radio Frequency Interference Suppression," PhD. Dissertation, The Ohio State University.
10. Hatke, G.F. and Phuong, T.T., 2004, "Design and Test of a GPS Adaptive Antenna Array Processor: The Multipath Adaptive Multibeam Array (MAMBA) Processor," Lincoln Laboratory Project Report GPS-16, Massachusetts Institute of Technology.
11. Fante, R.L., Fitzgibbons, M.P., and McDonald, K.F., 2004, "Effect of Adaptive Array Processing on GPS Signal Crosscorrelation," *Proc. ION GNSS 2004*, pp. 579-583.
12. McGraw, G.A., Ryan Youg, S.Y., and Reichenauer, K., 2004, "Evaluation of GPS Anti-Jam System Effects on Pseudorange and Carrier Phase Measurements for Precision Approach and Landing," *Proc. ION GNSS 2004*, pp. 2742-2751.
13. Frost, O.L., 1972, "An Algorithm for Linearly Constrained Adaptive Array Processing," *Proc. IEEE*, vol. 60, no. 8, pp 926-935.
14. Applebaum, S.P., 1976, "Adaptive Arrays," *IEEE Trans. on Antennas and Propagation*, vol. 24, no. 5, pp 585-598.
15. Widrow, B., Mantey, P.E., Griffiths, L.J., and Goode, B.B., 1967, "Adaptive Antenna Systems," *Proc. IEEE*, vol. 55, no. 12, pp. 2143-2159.
16. Kim, U.S., 2005, "Analysis of Carrier Phase and Group Delay Biases Introduces by CRPA Hardware," *Proc. ION GNSS 2005*, in press.
17. NovAtel Inc., 2004, "SuperStar II User Manual."
18. Zarlink Semiconductor Inc., 2002, "Datasheet for GP2015 – GPS Receiver RF Front End."
19. Interactive Circuits and Systems Ltd., 2001, "ICS-650 Operating Manual."